International Journal for Modern Trends in Science and Technology
Volume 12, Issue 03, pages 01-08.
ISSN: 2455-3778 online
Available online at: http://www.ijmtst.com/vol12issue03.html
DOI: https://doi.org/10.5281/zenodo.18870835

Design and Performance Analysis of PCF-SPR Biosensor for Skin and Adrenal Gland Cancer Detection

Venkatrao Palacharla[1], Sai Santoshi Kancharla[2], Navya Sri Chittiprolu[2], Mallikharjuna Swamy Peyyala[2], Y S S G R K Nooka Babu Inti[2], Naga Sai Ajay Vemuri[2]

Department of ECE, Godavari Global University, Rajamahendravaram, INDIA.
Department of ECE, Godavari Institute of Engineering & Technology (A), Rajamahendravaram, INDIA

To Cite this Article
Venkatrao Palacharla, Sai Santoshi Kancharla, Navya Sri Chittiprolu, Mallikharjuna Swamy Peyyala, Y S S G R K Nooka Babu Inti & Naga Sai Ajay Vemuri (2026). Design and Performance Analysis of PCF-SPR Biosensor for Skin and Adrenal Gland Cancer Detection, 12(03), 01-08. https://doi.org/10.5281/zenodo.18870835

Article Info
Received: 28 January 2026; Revised: 26 February 2026; Accepted: 02 March 2026.

KEYWORDS

SPR(Surface-Plasmon-Resonance), PCF(photonic-crystal-fiber), Biosensor, Cancer detection, Refractive index, FEM (finite-element-method), Wavelength Sensitivity, Amplitude Sensitivity.

ABSTRACT

We introduced a Highly sensitive Double-core Photonic Crystal Fiber Surface Plasmon Resonance biosensor to be used for an early-stage detection of skin and adrenal gland cancer. The Numerical Analysis is Performed using the finite element method in the COMSOL Multiphysics Software, with the aid of perfectly matched layers (to achieve satisfactory field absorption. The proposed biosensor has a circular air-hole shape with a bilayer plasmonic coating of Gold (Au) and Titanium dioxide (TiO2). Gold is chosen because of its high plasmonic activity, chemical stability, and strong resonance response, and TiO2 improves adhesion and mode coupling at the metal-dielectric interface. The dual-core structure also significantly enhances the coupling efficiency and the confinement of the electromagnetic field. Variations in refractive indices of healthy and cancerous Basal (skin) and PC12 (adrenal gland) cells are used to test the performance of the sensor. Several important performance metrics such as Resolution, Wavelength sensitivity, Figure of Merit (FOM) and Amplitude Sensitivity are greatly enhanced. The results ensure that the introduced PCF-SPR biosensor is a very compact and highly sensitive platform for early-stage cancer detection.

1. INTRODUCTION

Cancer is still one of the most critical health issues worldwide and it is responsible for large number of deaths every year according to the World Health Organization [1] Cancerous and normal cells have many differences, including biochemistry, morphology, and refractive index (RI) in particular. These variations in RI produce a natural optical contrast which may be exploited for rapid, label-free sensing. Hence, a number of optical based sensing techniques such as Photonic

Crystal Fibers and Surface Plasmon Resonance have been proven to be efficient in detecting cancer related abnormalities. SPR is especially powerful because it enables molecular interactions to be observed live in real time without the need for any fluorescent or chemical labels. The development of SPR technology started with Otto in the year 1968, who demonstrated that light can excite surface plasmons, and was further developed by Kretschmann and Raether in 1971 through the first practical metal film SPR configuration. Therefore, PCF-SPR biosensors can detect minute variation in RI, which makes them of great interest for advanced cancer detection, biomarker sensing, and other diagnostic applications.

Ayushman, Ramola et al. (2021) [2] introduces an external coated PCF based Surface Plasmon Resonance biosensor for the identification of several cancer cells. The dual-lattice PCF structure adopts the air-holes sizes $d_1 = 0.25\Lambda$ and $d_2 = 0.45\Lambda$ with a pitch of 2 μm, and the outer surface is covered with gold layer thickness 45 nm and an 85 nm titanium dioxide (TiO_2) layer. The parameters including Amplitude Sensitivity, Resolution, Wavelength Sensitivity, Figure of Merit (FOM) were investigated in the in COMSOL Multiphysics with FEM and a 2-μm PML. The sensor result showed out-standingly high sensitivity of 14,285.71 nm/RIU (TE mode) and 12,857.14 nm/RIU (TM mode), whereas the maximum amplitude sensitivity where achieved value of 15,010 RIU^{-1} (TE) and 13,240 RIU^{-1} (TM). The design also realized a quite small resolution of 7×10−6 RIU and a large FOM of 21.61 RIU^{-1}. This configuration demonstrates the potential role of Tio_2 and gold layers in enhancing the plasmonics for cancer biosensing applications.

Khalid Mohd Ibrahimi et al. (2023) [3] presented a SPR biosensor employing a twin-core PCF Configuration for the early identification of cancerous cells. The PCF structure is developed with hexagonal pattern with three distinct air-hole diameters 0.38 μm, 0.75 μm, and 1.45 μm at a fixed pitch 1.8 μm. A 1.3 μm analyte channel is located adjacent to the plasmonic zone for enhanced interaction with guided light. The plasmonic interface which is a 25 nm gold (Au) film capped with 12 nm TiO_2 adhesion layer, increases plasmon resonance intensity and chemical stability. A 1.50 μm PML layer is applied in the FEM analysis in COMSOL. The sensor attained a maximum As of 4285.71 RIU^{-1} and Ws of 4078.43 nm/RIU with a resolution of 4×10^{-5} RIU.

Arefe Ehyaee et al. (2023) [4] investigates a dual-core PCF refractive index sensor tailored for simultaneous multiple cancer cell sensing absence of metal-based SPR coatings. The structure comprises three circular rings of air holes with diameters of 2 μm (outer), 2.8 μm (middle), and 1.6 μm (inner) and has a central analyte channel of 3.6 μm. A pitch of 3 μm is retained throughout the lattice that provides sense of strong coupling between the two cores. The refractive indices of the infected cells, which implies Jurkat, PC12, Basal, MCF-7, MDA-MB-231 and Hela were investigated via FEM-based mode analysis. The sensor obtained excellent wave length sensitivity of 12,857.14 nm/RIU (PC12), 12,500 nm/RIU (MCF-7), 11,250 nm/RIU (HeLa) and maximum resolution of 8 × 10−6 RIU. Even though the proposed design does not involve plasmonic materials, the dual-core mechanism results in considerable spectral shifts, proving its viability for precise RI-based cancer detection.

Sonia Akter and Hasan Abdullah (2024) [5] proposed a gold covered circular PCF SPR biosensor for high RI sensitivity in cancer detection. The pattern consists of several circular air-hole rings with two different hole radii 0.7 μm and 0.8 μm, and a pitch of 4.1 to 4.7 μm. The outer layer is deposited by a 50 nm Au plasmonic layer with enhanced resonance properties. Two-dimensional FEM simulations were conducted for the refractive index in between 1.380 and 1.401, with a PML used as the absorber of the outward waves. The sensor demonstrated outstanding performance with a maximum Ws of 13257.20 nm/RIU, FOM of 36.52 RIU^{-1}, and a large birefringence value of 8.3×10^{-4}. The up-scaled Au layer and the circular placement of analyte led to strong plasmon excitation and magnified detection sensitivity for RI-based biomedical sensing.

B. Nagavel et al. (2024) [6] introduced a dual-core bilateral-surface PCF-SPR biosensor to sense the RI changes of various cancer cells. The Design uses circular cladding air holes of two diameters 0.80 μm and 1.60 μm arranged radially around the core with a pitch of 2.0 μm. A 40 nm gold overlaid on both sides of the dual-core region to form bilateral plasmonic coupling and thus the resonance interaction within the two plasmonic waveguide cores is strengthened. Based on FEM simulations, the sensor also exhibited more susceptibility

in breast cancer cell detection. It reached a Ws of 5714.28 nm/RIU, As of 899.248 RIU^{-1} with a resolution of 3.33×10^{-5} RIU. The symmetrical design facilitated stronger light – plasmon interactions and delivered better sensing results than those obtained from the conventional single-surface SPR sensor.

II. Structural Modelling and Theoretical Analysis

The numerical identification and modal study of the recommend biosensor were performed using the finite element method in the software package COMSOL Multiphysics (Version 5.4). The FEM is well known important and accurate numerical simulation tool for the analysis of complex optical waveguide designs, as it can efficiently solve partial differential equations, including Maxwell's equations with high accuracy.

The Operating Mechanism of proposed sensor is that of the Surface Plasmon Resonance (SPR). Light waves travel through the core of the PCF via modified Total Internal Reflection; in contrast, the presence of air spaces leads to a part of the optical field protruding into the cladding region as an evanescent wave. At this point of phase matching, the maximum energy transfer occurs from the core mode to the plasmonic mode, leading to a strong peak in the confinement loss spectrum. The resonance wavelength at this point strongly depends on the refractive index of the biological sample in the sensing area, thus facilitating the detection of cancerous cells. Extensive studies have looked into how geometric parameters, such as the type of metal layer, thickness, positioning, and the size and number of air holes effect sensor performance [7–10].

In proposed Sensor Geometry the cladding exists of air holes in a circular lattice. Here, the center-to-center spacing between adjacent air holes, referred to as the Pitch(P), which is taken as 1.6μm from table1. The pitch determines the mode confinement and the single mode operation of the fiber. Concentric Air-Hole Arrangement the design under investigation consists of three different-sized air holes. The smallest air holes have a diameter of 0.58μm, provide strong confinement of light within the core-guided region. The central ring contains air holes of diameter 0.92μm,which serves as a transitional layer to regulate evanescent field leakage. The biggest air holes are the outermost ones, with diameter 1.25μm.

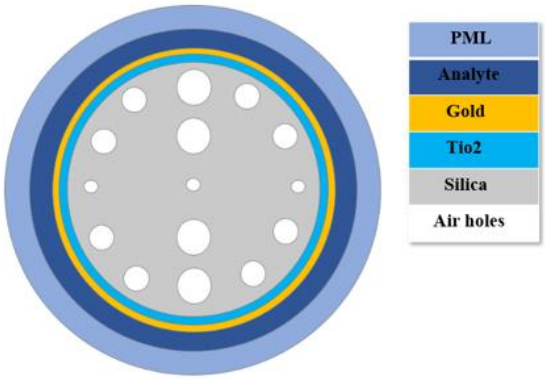

Fig. 1 Schematic representation of Proposed design

The gold (Au) layer is selected as the main plasmonic material owing to its chemical stability and bio-environmental non-oxidizability. Among available metals gold and silver are used most frequently [11]. The gold layer thickness (t_g) is set to 25 nano meters. However, adhesion of gold to silica fiber is weak. To overcome this a thin film of Titanium Dioxide (TiO_2) is first deposit between the silica and the gold film. The TiO_2 layer thickness (t_t) is fixed at 25[nm]. The analyte layer is of great importance since it mainly defines the sensing capability of the sensor with respect to different biological samples. The analyte layer (t_a = 1.3 μm) is situated very close to the plasmonic gold surface to maximize the overlap of the evanescent field with the target biological media.

PML was applied at the outermost boundary design [12]. It is a critical component in PCF simulations as it efficiently absorbs the radiative energy leaking from the core, thereby allowing for the accurate calculation of confinement loss. For this proposed design, the PML thickness is optimized from the table1.

Table1: Geometry of the Proposed biosensor

Parameter	Symbol	Value
Pitch	P	1.6[μm]
Inner hole diameter	D_1	0.58[μm]
Middle hole diameter	D_2	0.92[μm]
Outer hole diameter	D_3	1.25[μm]
Thickness of TiO_2	tt	25[nm]
Thickness of Gold	tg	25[nm]
Thickness of Analyte	ta	1.3[μm]
Thickness of PML	PML	1.5[μm]

III. Conceptual Analysis

The proposed sensor allows for the excitation of various optical modes, such as surface plasmon modes, core-guided modes, and transmission modes, as well as two well-confined orthogonal modes polarized in the x- and y-directions. Fused silica is chosen as the background material for the PCF structure owing to its low propagation loss, high chemical stability, and high optical transparency. The refractive index of fused silica is modeled using the Sellmeier equation [13]. This allows for a detailed simulation of modal propagation, phase matching, and surface plasmon resonance excitation in the proposed PCF-SPR biosensor.

$$n^2_{silica}(\lambda) = 1 + \frac{0.6961663\,\lambda^2}{\lambda^2-(0.0684043)^2} + \frac{0.4079426\,\lambda^2}{\lambda^2-(0.1162414)^2} + \frac{0.8974794\,\lambda^2}{\lambda^2-(9.896161)^2} \quad (1)$$

n_{silica} is the ReI of quartz glass and operating wavelength denoted by λ in micrometers (μm).
It's optical constants are extracted by fitting the Drude–Lorentz model and for that equation is given as [14], which leads to the accurate calculation of the permittivity and allows for an accurate simulation of the SPP along the gold–analyte interface.

$$\varepsilon_{Au}(\omega) = \varepsilon_\infty - \frac{\omega_D^2}{\omega(\omega+i\,\gamma_D)} - \frac{\Delta\epsilon.\Omega_L^2}{(\omega^2-\Omega_L^2)-i\,\Gamma_L\omega} \quad (2)$$

Where,
$\varepsilon_\infty = 5.9673$, $\omega = (2\pi c)/\lambda$, $\omega_D = (2113.60 \times 2\pi)$, $\gamma_D = (15.920 \times 2\pi)$ THz, $\Delta\varepsilon = 01.09$, $\Omega_L = (650.07 \times 2\pi)$, $\Gamma_L = (104.86 \times 2\pi)$

TiO_2 is introduced as an adhesion and high index buffer layer between silica and Au for the coupling efficiency improvement. Its refractive index is calculated by a dispersion relation of TiO_2. This layer enhances field confinement, blocks gold delamination, and bolsters plasmonic coupling to achieve high sensitivity and good repeatability. The refractive index dispersion of isotropic TiO_2 is estimated using the respective analytical formula given in [15].

$$n^2_{TiO2}(\lambda) = 5.913 + \frac{2.441\times10^7}{(\lambda^2-0.803\times10^7)} \quad (3)$$

The relative refractive indices of normal and cancerous cells are provided in Table 2.

Table2: Normal and Infected Cancer cells differ in refractive indices.

Cancer	Associated Cell	Refractive index (RI)		Change in RI	References
		Healthy cell	Cancerous cell		
Adrenal gland	PC12	1.3810	1.3950	0.024	[3]
Skin	Basal cell	1.3600	1.3800	0.014	[3]

Confinement loss denotes that portion of energy leaked from the guided core mode into surface plasmon polariton mode. It is calculated from the unreal part of the effective index of refraction. A sharp peak of the CL means phase matching and resonance. By following this peak through the analyte refractive indices, one can achieve good sensitivity for the detection of biomolecular changes. The confinement-loss is calculated using the following equation [16].

$$\alpha_{loss}\left(\frac{dB}{cm}\right) = 8.856 \times \frac{2\pi}{\lambda} \times img(n_{eff})10^4 \quad (4)$$

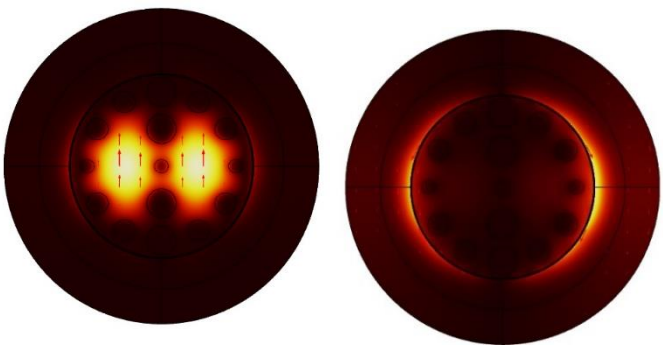

Fig. 2 Electric Field distributions of **(a)** core mode and **(b)** SPP-mode for optimal settings

Wavelength sensitivity quantifies the changing rate of the SPR resonance wavelength against the refractive index of the analyte. It is explained as the amount of resonance-wavelength shift for a given RI change. Strong plasmonic coupling shown in fig.2 corresponds to high sensitivity, and in PCF-SPR configurations this translates into higher early recognition of infected cells. Sensitivity using the wavelength interrogation (WI) method can be evaluated using Eq. [17].

$$S_w(\lambda) = \frac{\Delta\lambda_{peak}}{\Delta n_a}[nm/RIU] \qquad (5)$$

Here, Δn_a is the difference in refractive index between two adjacent analytes, and $\Delta\lambda_{peak}$ is the corresponding variation in the resonance wavelength of the analytes.

Amplitude sensitivity measures the change in magnitude of CL at a given wavelength as a function of analyte RI. Greater amplitude sensitivity implies more energy transfer to the plasmonic mode, which is also useful in cancer detection since minor biomolecular changes lead to the change of RI. The As can be described using the following formula [18].

$$S_A(\lambda) = -\frac{1}{\alpha(\lambda,n_a)} \times \frac{\partial\propto(\lambda,n_a)}{\partial n_a}\ [RIU^{-1}] \qquad (6)$$

Resolution is determined as the tiniest detectable vary in refractive index that can be measured by the sensor. It is given by the ratio of the smallest detectable wavelength change to the wavelength sensitivity of sensor. A smaller value of resolution indicates better sensing capability. In cancer detection applications, higher resolution is required to detect the smallest changes in refractive index corresponding to abnormal cell structures. The resolution (R) of the proposed biosensor is given by the expression [19].

$$\text{Res}\ (\lambda) = \Delta n_a \times \frac{\Delta\lambda_{min}}{\Delta\lambda_{peak}}\ [\text{RIU}] \qquad (7)$$

The FOM characterizes the entire sensor performance through a tradeoff between the sensitivity in wavelength and the sharpness in resonance curve. A higher FOM implies a narrower FWHM width and a stronger discriminating ability, which are important for exact determination of cancerous cell signatures. The enhancement of the TiO_2–Au interface and PCF structure design can be directly related to the FOM optimization in the presented design.

$$\text{Figure of Merit} = \frac{S_\lambda}{\text{FWHM}}[\ \text{RIU}^{-1}] \qquad (8)$$

IV. Results and Discussions

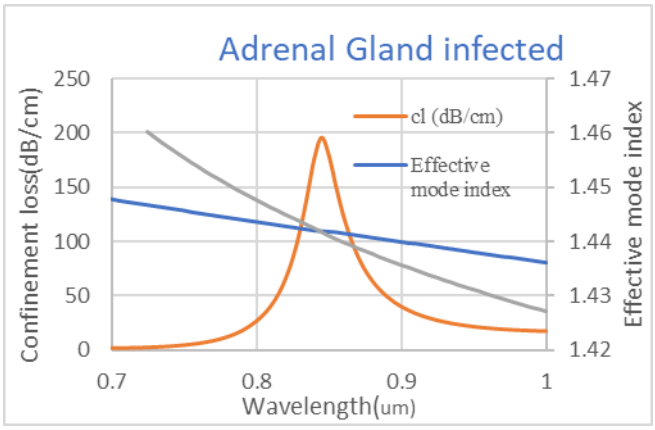

Fig. 3 Phase matching

We investigate the output of the suggested dual-core PCF-SPR biosensor for two cancers: Adrenal gland cancer (PC12 cells) and Skin cancer (Basal/Squamous cells). The sensor response is extracted by monitoring the confinement loss spectra for both normal and cancerous biomolecules. The results undoubtedly prove the strong excitation of surface plasmon resonance at Au/TiO_2 interface and show different resonance shifts due to the RI of bio-sample.

This graph shows the resonance condition for the infected skin cell, where the overlap of the effective indices of fundamental mode and Plasmon mode occurs at a wavelength of 955 nm. At this wavelength, the propagation loss also reaches its maximum value because of the increased energy transmit from fundamental mode to plasmon mode.

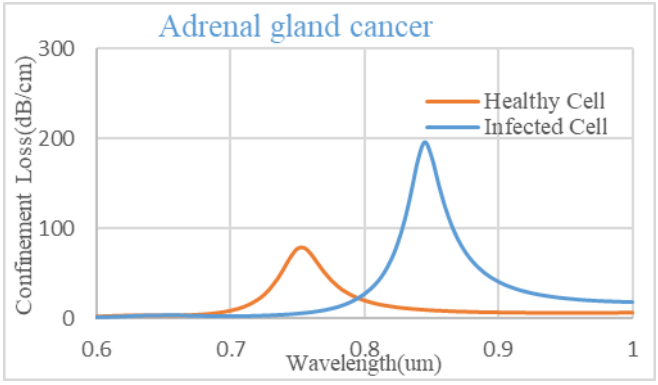

Fig.4 Wavelength shift of adrenal Gland Cancer

The Confinement Loss of normal and diseased adrenal gland cells are depicted in Fig.4. A substantial shift of the resonance wavelength for the infected case can be seen that validates strong RI-based coupling between the guided core mode and the plasmonic mode. The healthy cell results in a resonance at around 0.82 μm, while the infected cell yields a more pronounced and broader resonance around 0.95μm, suggesting increased plasmonic absorption due to elevated analyte RI.

As a consequence of resonance shift, sensor sensitivity in terms of wavelength is 6428.57 nm/RIU, which indicates good spectral responses to small changes in RI. An addition of confinement loss with rise of the RI of the analyte is implied by the amplitude sensitivity of -978.13 RIU^{-1}. The calculated Rs of 1.5×10^{-4} RIU verifies that sensor is capable of detecting minute molecular alterations that are associated with adrenal cancer progression.

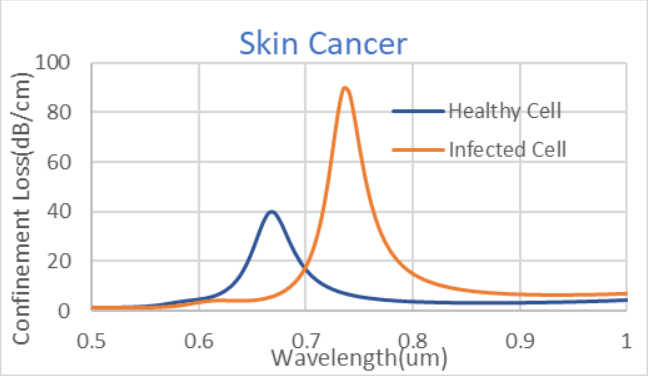

Fig.5 Wavelength shift of skin Cancer

The Figure 5 plots CL against wavelength for the healthy and infected skin layers. Similar to the adrenal case, the infected sample reveals a distinct redshift of the resonance peak from ~.72 micrometer (healthy) to ~0.80 μm (infected). The infected cell peak intensity is much larger, which means there is stronger mode coupling caused by the larger real part of the refractive index of the cancerous skin tissue.

Suggested sensor has wavelength sensitivity 3250 nm/RIU which is much less than that of the adrenal gland detection but is still quite high for the monitoring of biological RI. The −592.27 RIU−1 sensitivity corresponds to a uniform intensity change per unit RI increment.

The computed resolution of 3.07×10^{-4}RIU specifies that sensor can differentiate optical properties between normal and skin with cancer cells. More importantly, this sensor configuration possesses a high FOM of 65.00 which is the maximum among the two cases considered here, indicating that a sharper resonance and a stronger EM field will be obtained at the Au/TiO_2 interface.

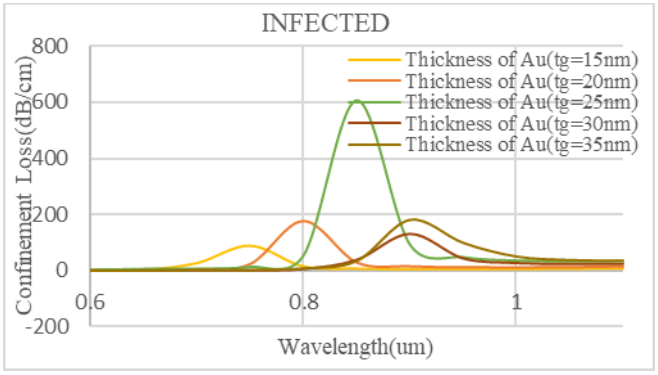

Fig.6 Dependence of confinement loss on gold layer thickness for adrenal gland cancer cells.

Figure 6 illustrates the effect of gold (Au) layer width on confinement loss spectrum of the preferred PCF-SPR biosensor for infected analyte. Gold thickness is varied from 15 nm to 35 nm to optimize plasmonic coupling. A pronounced resonance peak is observed at t_g = 25 nm, indicating maximum energy transfer between core mode and spp mode. Thinner Au layers result in weaker plasmon excitation due to insufficient electron density, while thicker layers reduce field penetration into the analyte, broadening resonance peak. Therefore, an optimized gold thickness is essential to achieve high sensitivity and strong SPR response.

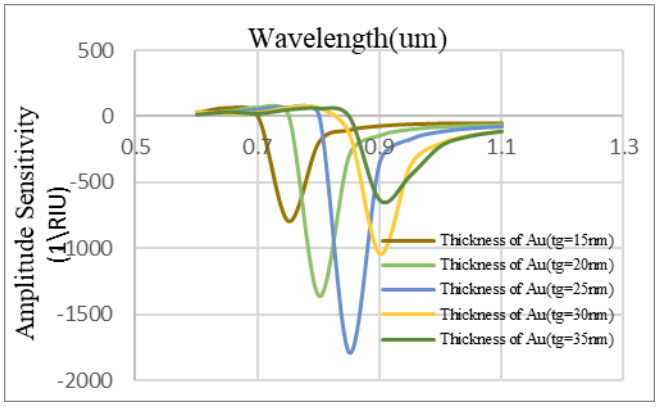

Fig .7 Amplitude sensitivity as a function of Au layer thickness for infected PC12 cancer cells.

The figure 7 presents the variation of gold layer thickness on amplitude sensitivity of the suggested PCF-SPR biosensor. Strong negative peaks occur at resonance wavelengths, indicating efficient surface plasmon coupling. Among all cases, an Au thickness of 25 nm produces the deepest amplitude sensitivity dip, confirming optimal plasmonic excitation and maximum energy transfer. Thinner Au layers (15–20 nm) show weaker responses due to insufficient free electron density, while thicker layers (30–35 nm) reduce sensitivity because of increased metallic damping and limited evanescent-field penetration. Thus, 25 nm gold thickness provides the best sensing performance.

V. CONCLUSION

The simulated bilayer dual-core PCF-SPR biosensor with a Titanium dioxide/gold layer is highly sensitive for detecting normal and cancerous bio samples due to changes in RI. The combined optimized circular analyte channel, multilayer plasmonic coating and enhanced dual-core mode coupling lead to strong SPR excitation with sharp confinement-loss peaks.

For the distinguish of adrenal gland cancer, the sensor exhibit a high wavelength sensitivity (6428.57 nm/RIU) and good detection resolution (1.5×10^{-4}RIU), which suggests a successful RI-dependent spectral discrimination. For skin cancer applications the sensor also demonstrates excellent FOM = (65 1/RIU) and good resonance separation which implies accurate and stable sensing.

In conclusion, the proposed PCF-SPR design could be a very reliable, compact and highly sensitive optical sensor for early cancer detection. The performance holds great promise to be incorporated in biomedical sensing, real-time cancer screening, and futuristic photonic diagnostic systems.

Table 3: Comparative Performance Analysis of the Proposed with Previously Reported Biosensors

Sensor	Cancerous cells	Ws (nm/RIU)	As (1/RIU)	Sr (RIU)	FOM (1/RIU)	References
Twin-core PCF SPR	PC12	3571.42	-2537.37	2.80×10^{-5}	-	[3]
	Basal cell	2500.00	-1611.02	4.00×10^{-5}	-	
C-shaped PCF SPR	PC12	1428.57	-489.66	7.00×10^{-5}	-	[22]
	Basal cell	1500.00	-447.97	6.70×10^{-5}	-	
Twin-core PCF SPR	PC12	4285.72	-750.443	2.33×10^{-5}	-	[6]
	Basal cell	3000.00	-360.236	3.33×10^{-5}	-	
Hexagonal PCF SPR	PC12	5714.29	-2361.97	1.75×10^{-5}	-	[20]
	Basal cell	3000.00	-1877.25	3.33×10^{-5}	-	
PCF-SPR	PC12	5500.00	-399	1.80×10^{-5}	-	[21]
	Basal cell	3150.00	-625	3.20×10^{-5}	-	
Twin-core PCF SPR	PC12	6428.57	-978.13	1.5×10^{-4}	142.85	Proposed work
	Basal cell	3250.00	-592.27	3.07×10^{-4}	65.00	

Conflict of interest statement

Authors declare that they do not have any conflict of interest.

REFERENCES

[1] https:// www. who. int/ news- room/ fact- sheets/ detail/ cancer.

[2] Ramola, A., Marwaha, A. & Singh, S. Design and investigation of a dedicated PCF SPR biosensor for CANCER exposure employing external sensing. Appl. Phys. A 127, 643 (2021). https://doi.org/10.1007/s00339-021-04785-2

[3] Ibrahimi, K.M., Kumar, R. & Pakhira, W. Enhance the Design and Performance Analysis of a Highly Sensitive Twin-Core PCF SPR Biosensor with Gold Plating for the Early Detection of Cancer Cells. Plasmonics 18, 995–1006 (2023). https://doi.org/10.1007/s11468-023-01825-w

[4] Ehyaee, A., Mohammadi, M., Seifouri, M. et al. Design and numerical investigation of a dual-core photonic crystal fiber refractive index sensor for cancer cells detection. Eur. Phys. J. Plus 138, 129 (2023). https://doi.org/10.1140/epjp/s13360-023-03749-0

[5] Akter, S., Abdullah, H. Design and Investigation of High-Sensitivity PCF SPR Biosensor for Various Cancer Cells Detection Using a Gold-Coated Circular-Shaped Structure. Plasmonics 20, 5303–5313 (2024). https://doi.org/10.1007/s11468-024-02727-1

[6] B, N., Dagar, H. & Krishnan, P. High-Performance Dual-Core Bilateral Surface Optimized PCF SPR Biosensor for Early Detection of Six Distinct Cancer Cells. Plasmonics 20, 4799–4809 (2024). https://doi.org/10.1007/s11468-024-02661-2

[7] Dash JN, Das R, Jha R (2018) AZO coated microchannel incorporated PCF-based SPR sensor: a numerical analysis. IEEE Photon Technol Lett 30.11:1032–1035 9.

[8] Jiang G, Yanjun Fu, Huang Y (2015) High birefringence rectangular-hole photonic crystal fiber. Opt Fiber Technol 26:163–171 10.

[9] SM A et al (2007) Design of a decagonal photonic crystal fiber for ultra-flattened chromatic dispersion. IEICE Trans Electron 90.11:2141–2145 11.

[10] Yasli A, Ademgil H (2018) Geometrical comparison of photonic crystal fiber-based surface plasmon resonance sensors. Opt Eng 57(3):030801

[11] Dash, JN, Jha R (2014) SPR biosensor based on polymer PCF coated with conducting metal oxide. IEEE Photon Technol Lett 26.6:595–598

[12] Wang H et al (2021) A dual-channel surface plasmon resonance sensor based on dual-polarized photonic crystal fiber for ultra-wide range and high sensitivity of refractive index detection. IEEE Photon J 13.1: 1–11

[13] Ahmed K, Jabin Md, Paul BK (2020) Surface plasmon resonance-based gold-coated biosensor for the detection of fuel adulteration. J Comput Electron 19.1:321–332 16.

[14] Vial A et al (2005) Improved analytical fit of gold dispersion: application to the modeling of extinction spectra with a finite difference time-domain method. Phys Rev B 71.8:085416

[15] DeVore JR (1951) Refractive indices of rutile and sphalerite. JOSA 41.6:416–419 19.

[16] Jahan N et al (2021) Photonic crystal fiber-based biosensor for pseudomonas bacteria detection: a simulation study. IEEE Access 9:42206–42215 20.

[17] Sakib MN et al (2020) Numerical study of circularly slotted highly sensitive plasmonic biosensor: a novel approach. Results Phys 17:103130 22.

[18] Islam MR et al (2020) Dual-polarized highly sensitive surface plasmon-resonance-based chemical and biomolecular sensor. Appl Opt 59.11:3296–3305 21.

[19] Wang G et al (2016) Highly sensitive D-shaped photonic crystal f iber biological sensors based on surface plasmon resonance. Opt Quantum Electron 48.1:1–9

[20] Ibrahimi, K.M., Kumar, R. & Pakhira, W. C-grooved dual-core PCF SPR biosensor with graphene/au coating for enhanced early cancer cell detection. Appl. Phys. A 130, 439 (2024). https://doi.org/10.1007/s00339-024-07593-6

[21] Ibrahimi, K.M., Kumar, R. & Pakhira, W. Early detection of cancer cells using high-sensitivity dual-side polished photonic crystal fiber biosensors based on surface plasmon resonance. Opt Quant Electron 56, 888 (2024). https://doi.org/10.1007/s11082-024-06782-0

[22] Ibrahimi KM, Kumar R, Pakhira W (2024) C-grooved dual-core PCF SPR biosensor with graphene/au coating for enhanced early cancer cell detection. Appl Phys A 130:439